Fine Structure of the N=1 (1s3p)3Πu State of the Hydrogen Molecule Determined by Magnetic Resonance

R. Jost, M. A. Marechal, M. Lombardi

(1970).
[34]M. Lombardi (unpublished).
[35]G. H. Dieke, S. P. Cunnigham, and F. T. Byrne, Phys. Rev. 92, 81 (1953).

PHYSICAL REVIEW A VOLUME 5, NUMBER 2 FEBRUARY 1972

Fine Structure of the $N = 1$ $(1s3p)$ $^3\Pi_u$ State of the Hydrogen Molecule Determined by Magnetic Resonance

R. Jost, M. A. Marechal, and M. Lombardi
Université Scientifique et Médicale de Grenoble, Laboratoire de Spectrométrie Physique, CEDEX-53, Grenoble-Gare 38, France
(Received 28 July 1971)

In the preceding paper some of our results on the magnetic-resonance experiments performed at 64 MHz indicated a beginning of $\underline{N}\cdot\underline{S}$ decoupling on the $N=1$ $(1s3p)$ $^3\Pi_u$ state of H_2 excited by electron impact. In the present paper we present further results on the resonance experiments performed at higher frequencies in order to determine the fine structure of this level. Our findings indicate that the energy separation between $J=1$ and $J=2$ levels is 160 ± 5 MHz and between $J=1$ and $J=0$ levels it is 2100 ± 600 MHz, and in addition the former exhibits a small dependence on the vibrational number. The relative order of these levels is $J=1, 2, 0$ instead of the theoretically predicted 2, 1, 0. The Landé g factor is 1.249 ± 0.010, which corresponds to a pure Hund's-coupling case (b).

I. INTRODUCTION

As was suggested in Paper I,[1] a study of the Bitter-Brossel resonance[2] as a function of frequency is performed on the optical transition ($\lambda = 5994$ Å) arising from the $(1s3p)$ $^3\Pi_u$ ($v=0$, $N=1, S=1$, $I=0$) state of H_2. This resonance, previously carried out at 21, 35, and 64 MHz, is extended to 105 and 147.6 MHz where the $\underline{N}\cdot\underline{S}$ decoupling is strong enough to separate the different resonances due to the Zeeman sublevels. The study of the position and the intensity of the resonances at 147.6 MHz enables us to deduce the following information about the fine structure of the level: the energy separation between the $J=1$ and $J=2$ levels, an order of magnitude of the energy of the $J=0$ level, and the relative disposition of those three levels.

Similar work has been performed[3,4] on the $2\,^3P$ and $3\,^3P$ levels of He^4. Our present theoretical treatment is similar to the one of Lamb,[3] except for the intensity calculation. On the other hand, experimental conditions are more difficult than those of Ref. (4) (the lifetime τ of the studied level is three times shorter, the fine structure four times smaller, and the observed intensity is roughly 1000 times weaker in our case).

An extension of this experimental work at the next three vibrational (v) levels of the same electronic and rotational state enables us to estimate the dependence of the fine structure on v. We have also deduced from this study the Landé g factor of this state at zero magnetic field.

A level-crossing experiment at nonzero magnetic field[5] may also be used to determine the magnitude of the fine structure. Such an experiment, currently being performed in our laboratory has given preliminary results[6,7] which are in agreement with those reported here.

II. EXPERIMENTAL

The experimental setup for the excitation of H_2 and for the detection of the signal is the same as described in Paper I. At 105 MHz, as for 64 MHz,[1] the resolution of the resonances from the different Zeeman sublevels is not sufficiently good to justify precise measurements.

We present in Fig. 1 a resonance curve obtained at 147.6 MHz in the region of 60–180 Oe. We can see on this figure the continuous base line becoming increasingly curved with the magnetic field. The evaluation of the relative heights of the resonances depends on the determination of this base line. The shape of the base line which was found to be unchanged in the absence of rf field can be explained as follows: (i) a level anticrossing[3] whose shape is the same as our base line; this effect exists even for constant excitation process, i.e., $Q_0 - Q_1 = \text{const}$ (see Appendix); (ii) a possible continuous change in the excitation process due to the modification of the electron trajectory by the static magnetic field which implies that $Q_0 - Q_1$ is a function of H_z; (iii) a continuous change in the total emitted intensity with the magnetic field which can be as high as 30% and is only partially compensated by the detection system.[8]

The experimental resonance curves obtained at 35, 64, and 147.6 MHz are reproduced in Fig. 2, the base line being subtracted. The observations were repeated several times to verify the reproducibility of the measurements.

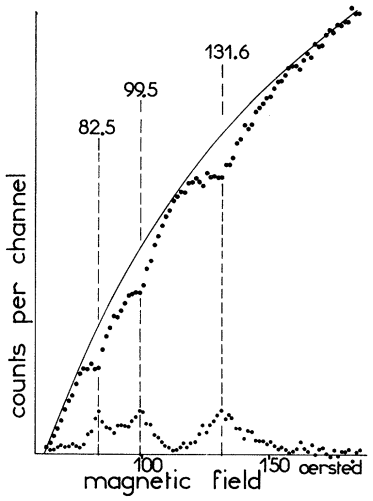

FIG. 1. Experimentally observed resonances on the 5994-Å line at 147.6 MHz. This measurement required 20 h of multichannel accumulation. The shape of the continuous baseline (drawn in full line) was checked by comparison with the baseline obtained in the absence of rf field. The lower curve is the negative of the upper curve after the baseline is subtracted. The centers of the resonances are determined with a precision of 1 Oe.

III. DISCUSSION

From a consideration of the Chiu calculation[9] one can show that the energy separation between the $J=1$ and $J=2$ levels is much smaller than the energy separation between the $J=0$ and $J=1$ levels. Then, in order to interpret the above experimental results, we have to plot an energy diagram for the $J=1$ and $J=2$ levels, evaluate the correction due to the existence of the $J=0$ level on the position of the Zeeman sublevels ($J=1$, $M_J=0$; $J=2$, $M_J=0$), calculate the theoretical ratio of the relative intensity of the resonances as a function of the static magnetic field where the transitions occur, and determine the energy separation of the levels $J=0$, 1 and 2 which best fit the experimental results. These separate steps are considered in subsections A, B, C, and D below.

In the following calculations we start with unperturbed wave functions given by a pure Hund's-coupling case (b),[10] which we call $|SN\Lambda, JM_J\rangle$. This is justified by the fact that the Landé g factor (1.235) found at the lowest frequency (21 MHz) is very close to the theoretical value in a pure Hund's case (b) (1.251). If the final extrapolated value at zero magnetic field (when no pure $\underline{N}\cdot\underline{S}$ decoupling occurs) is significantly different from 1.251, a correction to this b-coupling scheme should be applied.

A. Construction of the Energy Level Diagram

In zero magnetic field the energy of a $|SN\Lambda J\rangle$ level of a $^3\Pi_u$ state is given by[9,11]

$$E_J = \langle S=1, N, \Lambda=1, J | \mathcal{H}_{fs} | S=1, N, \Lambda=1, J\rangle$$

$$= \frac{AC}{2N(N+1)} + [(N^2+N-3)B_0 \mp (\tfrac{3}{2})^{1/2} N(N+1) B_2] \times \frac{3C(C+1) - 8N(N+1)}{4N(N+1)(2N-1)(2N+3)} , \quad (1)$$

where

$$C = J(J+1) - N(N+1) - 2 .$$

The fs subscript denotes fine structure, the minus sign applies to odd rotational levels in para-H_2, A is the spin orbit and spin-other-orbit coupling constant, and B_0 and B_2 are the spin-spin coupling constants.

In the following calculation the energy E_J of the $J=1$, 2, and 0 levels is taken respectively equal to $-\frac{5}{8}\alpha$, $+\frac{3}{8}\alpha$, β, with $\alpha \ll \beta$.

When a static magnetic field H_Z is applied, the Zeeman energy is given by the eigenvalue $\lambda_{JM_J J'M'_{J'}}$ of the matrix

$$\langle SN\Lambda, JM_J | (\hbar|e|/2mc) H_Z (\underline{L}_Z + 2\underline{S}_Z) + \mathcal{H}_{fs} | SN\Lambda, J'M'_{J'}\rangle = f(H_Z, SN\Lambda J J' M_J M'_{J'}) \delta(M_J M'_{J'}) .$$

This energy is plotted as a function of the dimensionless number (decoupling parameter) $\chi = (\hbar|e|/2mc\alpha)H_Z$ for the two levels $J=1$ and 2 in Fig. 2. The eigenfunctions are written $|i\rangle = |SN\Lambda, JM_J\rangle$. We present here the submatrix corresponding to $M_J = M'_{J'} = 0$ whence we deduce the energies λ_J of the $M_J = 0$ sublevels and the corresponding eigenfunctions in the limit $\beta/\alpha \to \infty$:

$$\begin{array}{c} J \quad 0 \qquad\quad 1 \qquad\quad 2 \\ \begin{pmatrix} 0 & +\beta/\alpha & (\frac{3}{2})^{1/2}\chi & 0 \\ 1 & (\frac{3}{2})^{1/2}\chi & -\frac{5}{8} & (\frac{3}{2})^{1/2}\chi \\ 2 & 0 & (\frac{3}{2})^{1/2}\chi & \frac{3}{8} \end{pmatrix} ; \end{array}$$

$$\lambda_{(J=1)}^{(J=2)} = -\tfrac{1}{8} \pm \tfrac{1}{2}(1+3\chi^2)^{1/2} , \quad (2)$$

$$|111, J=1 M_J=0\rangle = \cos\theta\,|111,10\rangle - \sin\theta\,|111,20\rangle ,$$
$$|111, J=2 M_J=0\rangle = \sin\theta\,|111,10\rangle + \cos\theta\,|111,20\rangle , \quad (3)$$

$$\tan\theta = \frac{(1+3\chi^2)^{1/2}-1}{\chi\sqrt{3}} \quad \text{with } 0 \le \theta \le \tfrac{1}{4}\pi .$$

In such a Zeeman diagram we can see that for a given frequency ν the transition $|111,21) \rightarrow |111,20)$ coincides with $|111,10) \rightarrow |111,1-1)$, while $|111,20) \rightarrow |111,2-1)$ coincides with $|111,11) \rightarrow |111,10)$.

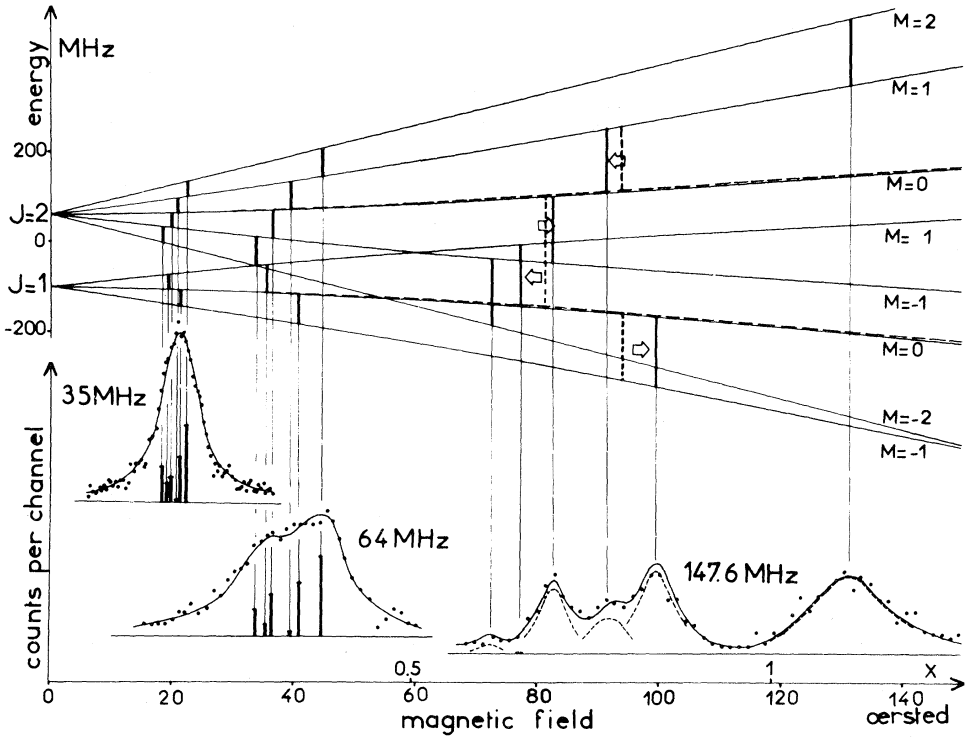

FIG. 2. Energy-level diagram for $J=1$ and 2 as a function of the magnetic field or of the $\underline{N}\cdot\underline{S}$ decoupling parameter $\chi=\hbar|e|H_Z/2mc\alpha$. This diagram corresponds to the following values: $g=1.25$, $\alpha=160$ MHz, $\beta=2000$ MHz. The positions and the intensities of the resonances (Table I) are shown for 35, 64, and 147.6 MHz. The dashed lines represent the $M_J=0$ energy levels and the transitions arising from these levels, calculated by neglecting the $J=0$ level, while the solid lines include this perturbation. The arrows show the direction of the displacement in these transitions due to the perturbation, the $(J=0)$ energy being assumed positive in this diagram. In the lower part of this figure the resonance curves due to these $\Delta J=0$ rf transitions are represented by circles. The reconstituted curves are drawn in solid lines; for this purpose, each resonance is represented by a Lorentzian centered at χ_0, of intensity I_0, and width ΔH_0 (Table I). At 35 and 64 MHz, we show only I_0 and the sum of these Lorentzians; at 147.6 MHz we represent by a dashed line each of these Lorentzians.

B. Correction Due to the Existence of the $J=0$ Level

When α is not negligible compared to β, the proximity of the $J=0$ level tends to repel the $|111, JM_J=0\rangle$ sublevels. Then the energy $\lambda_{JM_J=0}(\chi)$ of these sublevels is given by first order perturbation theory, where $\lambda^0_{JM_J=0}$ and θ are given by (2) and (3):

$$\lambda_{J=1}(\chi)=\lambda^0_{J=1}(\chi)+(\cos^2\theta)\,\frac{3}{2}\,\frac{\chi^2}{\lambda^0_{J=1}-\lambda^0_{J=0}}\,,$$

$$\lambda_{J=2}(\chi)=\lambda^0_{J=2}(\chi)+(\sin^2\theta)\,\frac{3}{2}\,\frac{\chi^2}{\lambda^0_{J=2}-\lambda^0_{J=0}}\,.$$

Such a displacement of the $|111, JM_J=0\rangle$ sublevels implies a change in the position of the resonances arising from these sublevels. More precisely, the previously superimposed transitions are now separated. The direction of the displacement is determined by the position of the $J=0$ level with respect to the $J=1$ and $J=2$ levels. The consequences of the correction are tabulated in Table I and represented in Fig. 2 at $\nu=147.6$ MHz for the determined parameters α and β.

C. Intensity of the Optical Resonance Line in the $\underline{N}\cdot\underline{S}$ Decoupling Zone

The calculation carried out in Paper I is no longer valid in the present case of partial $\underline{N}\cdot\underline{S}$ decoupling. We wish to express the intensity I of the light emitted by an optical transition connecting the initial state $|I\rangle=|SN\Lambda\rangle$ to the final state $|F\rangle=|S_0N_0\Lambda_0\rangle$ [the corresponding magnetic sublevels are written $|f)$] in the presence of an rf field, that is when a rf transition occurs between the $|i)$ and $|j)$ sublevels of $|I\rangle$. The calculation is carried out in the noncoupled basis

$$|i)=\sum_{M_SM_N} C^i_{M_SM_N}(\chi)\,|SM_S\rangle\,|NM_N\rangle\,.$$

The expression for $I(\vec{u},\lambda)$, the observed intensity, is[12]

$$I(\vec{u},\lambda)=I_0\,\mathrm{Tr}\,|\underline{\rho}(t)\,(\underline{e}_{\vec{u},\lambda}\cdot\underline{D})\,(\underline{e}_{\vec{u},\lambda}\cdot\underline{D})|\,, \qquad (4)$$

where $\underline{e}_{\vec{u},\lambda}$ is the polarization vector of the emitted

TABLE I. Characteristics of the resonances due to the $M_J \leftrightarrow M_J'$ rf transitions at different frequencies.

		$J=2$				$J=1$	
		$2 \leftrightarrow 1$	$1 \leftrightarrow 0$	$0 \leftrightarrow -1$	$-1 \leftrightarrow -2$	$1 \leftrightarrow 0$	$0 \leftrightarrow -1$
21 MHz	χ_0	0.110 78	0.107 00	0.103 64	0.100 73	0.102 36	0.108 30
	I_0 (a.u.)	0.356	0.020	0.098	0.225	0.106	0.195
	ΔH_0 (Oe)	6.15	6.12	6.08	6.05	6.08	6.12
35 MHz	χ_0	0.192 50	0.180 26	0.171 30	0.163 45	0.167 50	0.184 26
	I_0 (a.u.)	0.386	0.009	0.121	0.186	0.082	0.216
	ΔH_0 (Oe)	6.27	6.15	6.05	5.98	6.05	6.15
64 MHz	χ_0	0.3817	0.3370	0.3077	0.2840	0.2970	0.3494
	I_0 (a.u.)	0.383	0.014	0.193	0.119	0.045	0.246
	ΔH_0 (Oe)	6.95	6.36	5.88	5.45	5.88	6.64
147.6 MHz	$\chi_{0(\text{ump})}$[a]	1.1245	0.8000	0.6925	0.604	0.6925	0.8000
	χ_0	1.1245	0.7855	0.7000	0.604	0.6487	0.8500
	I_0 (a.u.)	0.281	0.130	0.245	0.033	0.001	0.310
	ΔH_0 (Oe)	13.9	6.95	5.45	4.25	5.65	6.95

[a]The centering $\chi_{0(\text{ump})}$ of the resonance is obtained by neglecting the perturbation resulting from the $J=0$ level.

light and $\underline{D}$ the electric dipole moment. The steady-state density matrix $\underline{\rho}(t)$ is

$$\underline{\rho}(t) = \int_{-\infty}^{t} e^{-\Gamma(t-t_0)}\, \underline{U}(t, t_0)\, \underline{\rho}(t_0)\, \underline{U}^{\dagger}(t, t_0)\, dt_0 \,. \qquad (5)$$

$\underline{\rho}(t_0)$ is the excitation density matrix and $\underline{U}(t, t_0)$ the evolution operator. This operator is given by second-order time-dependent perturbation theory[13] where the perturbation Hamiltonian is

$$\underline{\mathcal{H}}^{(1)} = \mu_B H_1 \left[(g_N \underline{N}_+ + g_S \underline{S}_+) e^{-i\omega t} + (g_N \underline{N}_- + g_S \underline{S}_-) e^{i\omega t}\right] .$$

The dc term of $I(\vec{u}, \lambda)$ of second order in H_1 is

$$\Delta I(\vec{u}, \lambda) = (\mu_B H_1)^2 \left[(i | g_N \underline{N}_+ + g_S \underline{S}_+ | j)\right]^2 \times (\rho_{ii} - \rho_{jj})(I_{ii} - I_{jj}) \,, \qquad (6)$$

where

$$I_{ii} = \sum_f (i | \underline{e}_{\vec{u},\lambda} \cdot \underline{D} | f)(f | \underline{e}_{\vec{u},\lambda} \cdot \underline{D} | i) \,.$$

To establish (6) we have taken into account the fact that we observe only $\Delta M_J = \pm 1$ rf transitions. This implies that neither the electronic excitation (parallel to the static magnetic field) nor the detection ($I_\pi - I_\sigma$) are coherent,[12] i.e., $\rho_{ij} = I_{ij} = 0$.

The calculation of $\Delta I(\vec{u}, \lambda)$ is performed for an I_π detected signal. Experimentally we detect the signal $I_\pi - I_\sigma$ which is proportional to ΔI_π. The calculation of I_{ii} is then simplified by the fact that the final level $|F\rangle$ is a $N=0$ level and we obtain

$$I_{ii} \propto \sum_{M_S} |C^i_{M_S, M_N=0}(\chi)|^2 \,.$$

The calculation of ρ_{ii} is simplified by the axial symmetry of the excitation and by the fact that the electronic excitation can be described as a product of an isotropic matrix in the spin space (S) and an anisotropic matrix in the orbital space (N).[14] We shall show (Appendix) that due to the fact that we observe a $N=1$ excited level, the ratio of the intensities of the various rf resonances is independent of the unknown cross sections of excitation of the various sublevels of $|I\rangle$. We obtain

$$\rho_{ii} \propto \sum_{M_S} |C^i_{M_S, M_N=0}(\chi)|^2 \,.$$

The calculation carried out by Lamb concerning the intensities of the resonances in the ^3P level ($J=0$, 1 and 2) of the He is similar to this one, except that our calculation is valid for any excitation density matrix instead of the particular one corresponding to the threshold excitation of He: The latter is not valid in our case.

We have plotted in Fig. 3 the calculated relative intensities of the different resonances lines corresponding to the $\Delta J = 0$ rf transitions as a function of χ the decoupling parameter. We have also evaluated the intensities of the $\Delta J = 1$ resonances for the 147.6 MHz frequency; but their weak intensities together combined with their large widths make them undetectable with the present signal to noise ratio.

D. Reconstitution of Spectra

We have finally three adjustable parameters, g, α, and β, to reconstitute the spectra obtained at 21, 35, 64, and 147.6 MHz. We proceed by successive approximations. As a first approximation we choose a g value of 1.25 corresponding to a pure Hund's-coupling case (b) which permits us to calculate the Zeeman diagram and determine the constants α and β. Then we evaluate the center of gravity of the resonance at 21 and 35 MHz, which gives us the deviation from the value 1.25 of the

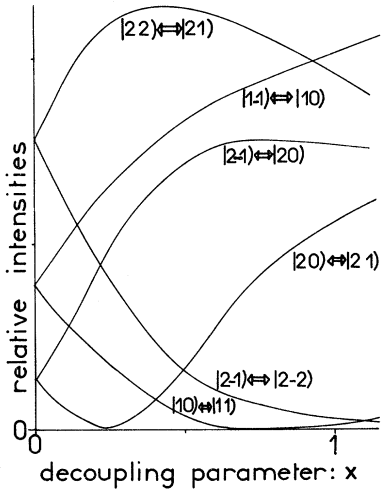

FIG. 3. Calculated relative intensities of the resonance curves for a ($S=1$, $N=1$, $\Lambda=1$) level as a function of the $\underline{N}\cdot\underline{S}$ decoupling parameter $\chi=\hbar\,|e|\,H_Z/2mc\alpha$. Each line represents the relative intensity of the resonance due to a ($\Delta J=0$, $\Delta M_J=\pm1$) rf transition between the sublevels $|S=1, N=1, \Lambda=1, JM_J)$. The calculation is carried out by neglecting the second-order perturbation due to the $J=0$ level.

Landé g factor measured at those frequencies due to the partial $\underline{N}\cdot\underline{S}$ decoupling. This deviation will allow us to deduce the Landé g factor at zero field from the experimentally measured g-value of the resonances at 21 and 35 MHz.[1]

The experiment shows that the relative order of the J levels is 1, 2, 0. The fine constants thus found,

$$\alpha=160\ \text{MHz},\quad \beta=2000\ \text{MHz}\ ,$$

are used as the basis of Table I. In this table are shown: the calculated resonance centers χ_0 as deduced from the Zeeman diagram corresponding to $g=1.25$, the calculated intensity I_0 at the center of the resonance (for convenience we have chosen $\sum I_0=1$), and the relative full width at half-maximum (FWHM) $\Delta H_0=(1.25/r)\,\Delta H_0'$, where r is the relative slope of the two sublevels; we have chosen $\Delta H_0'=6.1$ Oe, double the Hanle FWHM at zero pressure,[1,2] which corresponds to a zero rf field. Each of these quantities is calculated for different frequencies and shown in Fig. 2 for 35, 64, and 147.6 MHz.

In Fig. 4, we have plotted by a dashed line the theoretical resonance curve occurring at $\nu=35$ MHz when the $\underline{N}\cdot\underline{S}$ decoupling is neglected; this implies that the Lorentzian curve is centered at $\chi_1'=35/g\alpha$, with $g=1.25$, a height normalized to unity, and a width of $\Delta H_0'=6.1$ Oe. By means of a solid line we have plotted the resulting theoretical resonance profile taking into account the $\underline{N}\cdot\underline{S}$ decoupling; each resonance due to each rf transition $|111, JM_J)$ $\rightarrow$ $|111, JM_J')$ is represented by a Lorentzian characterized by χ_0, I_0, and ΔH_0 (Table I); the center of gravity χ_1 of this resulting curve corresponds to an apparently modified g factor $g_m=1.25-0.035$. A similar calculation for $\nu=21$ MHz gives $g_m=1.25-0.013$.

This permits us to deduce from the experimental measurements[1] the extrapolated zero-field g value:

$$(35\ \text{MHz})\ g=(1.215\pm0.010)+0.035=1.250\pm0.010\ ,$$

$$(21\ \text{MHz})\ g=(1.235\pm0.010)+0.013=1.248\pm0.010\ .$$

Moreover, we detect a broadening of 1.4 Oe in the reconstituted curve at 35 MHz and of 0.2 Oe at 21 MHz. This last result shows to a precision of 5% that we can neglect this broadening at 21 MHz in the evaluation of the b parameter defined in Paper I.

This above reconstitution is possible only within a certain range of α and β values determined by the experimental accuracy. The final values are

$$g=1.249\pm0.010,\quad \alpha=160\pm5\ \text{MHz},$$

$$\beta=2000\ {}^{+700}_{-500}\ \text{MHz}\ .$$

We have performed similar resonance experiments at 147.6 MHz on the upper vibrational levels ($N=1$, $I=0$) of the same electronic ($1s3p$) $^3\Pi_u$ state. The wave lengths of the observed optical transitions are 6098 ($v=1$), 6201 ($v=2$), and 6303 Å ($v=3$). The present results together with those found at low frequencies in Paper I give the same value for g within the experimental errors, and exhibit a de-

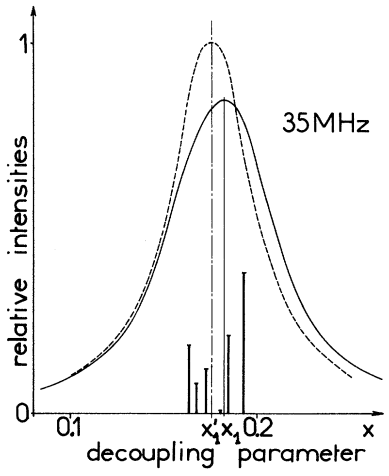

FIG. 4. Calculated resonances at 35 MHz on the ($S=1$, $N=1$, $\Lambda=1$) level assuming a pure Hund's-s-coupling case (b) ($g=1.25$). The resonances are represented by a dotted line for the case when the $\underline{N}\cdot\underline{S}$ decoupling is neglected and by a solid line when the $\underline{N}\cdot\underline{S}$ decoupling is taken into account using the fine structure parameter $\alpha=160$ MHz. The respective centers of gravity of these two curves are $\chi_1'=0.175\,47$ and $\chi_1=0.180\,60$.

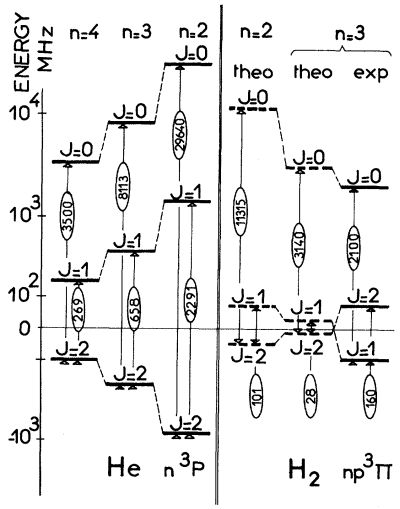

FIG. 5. Comparison between the $np\ ^3\Pi_u$, $N=1$ fine levels in parahydrogen and $np\ ^3P$ in ^{4}He. For the sake of legibility in both diagrams we drop an energy scale of the form: (sign of E)$\times \log_{10}(1+|E|)$. The origin of E is taken to be the center of gravity of the two fine levels $J=1$ and $J=2$, appropriately weighted. The values quoted for the He n^3P are taken from Lamb (Ref. 4) and Descoubes (Ref. 6). The levels in hydrogen shown as dotted lines are inferred theoretically (Ref. 9) for $n=2$ using the experimental results of Lichten (Ref. 15), while those for $n=3$ are obtained using the same scale reduction factor as between the $n=2$ and $n=3$ levels in He.

pendence of the parameter α on the vibrational level. We obtain: $\alpha = 160 \pm 12$ MHz (for $v=1$); $\alpha = 195 \pm 12$ MHz (for $v=2$); and $\alpha = 230 \pm 25$ MHz (for $v=3$). The above experimental accuracy is worse than for $v=0$ due to the proximity of optical transitions which necessitate a better resolution.

IV. CONCLUSION

The preceding experimental results concerning the $N=1$ level of the $(1s3p)\ ^3\Pi_u$ state of H_2 give the two parameters of the fine structure of this level (α, β) and the relative position $J=1, 2, 0$ of the fine levels. The experimental values of α and β can be expressed in terms of the physical constants A, B_0, and B_2 which are independent of N. By the use of (1) we obtain

$$\beta + \tfrac{3}{8}\alpha = E_0 - E_2 = -\tfrac{1}{2}A + \tfrac{9}{20}(-B_0 - \sqrt{6}\,B_2)$$

$$= +1940\ ^{+700}_{-500}\ \text{MHz},$$

$$\alpha = E_2 - E_1 = A + \tfrac{3}{10}(-B_0 - \sqrt{6}\,B_2)$$

$$= +160 \pm 5\ \text{MHz}.$$

In this evaluation we have fixed the position of the $J=0$ level as $E_0 > E_1, E_2$, using an extension of the work of Lichten,[15] Chiu,[9] and Fontana.[11] The lack of experimental precision does not allow us to determine accurately A and $(B_0 + \sqrt{6}\,B_2)$.

These results, concerning a molecular level without rotational energy, can be compared (Fig. 5) to those experimentally obtained on the $(1snp)$ of He [12,16] and to those concerning the $N=1$ $(1snp)$ of H_2. The $N=1$ $(1s2p)\ ^3\Pi_u$ of H_2 is obtained from the experimental A, B_0, and B_2 determination of Lichten.[15] The scaled $N=1$ $(1s3p)\ ^3\Pi_u$ of H_2 is obtained by extension of the preceding result using the fs variation law with n deduced from the He experimental results.

We can see that present measurement gives a result different from the one predicted by a simple scaling procedure.

APPENDIX

We wish to show that in the case of a $N=1$ level, the relative intensities of the resonances are independent of any excitation parameters.

For a $N=1$ level, assuming an electronic excitation of axial symmetry, the orbital part ${}^N\underline{\rho}(t_0)$ of the excitation density matrix is a 3×3 anisotropic matrix,

$$\begin{pmatrix} Q_1 & 0 & 0 \\ 0 & Q_0 & 0 \\ 0 & 0 & Q_{-1} \end{pmatrix}$$

which is a function of only two parameters, Q_0 and $Q_1 = Q_{-1}$, the excitation cross sections of the $M_N = 0$ and $M_N = \pm 1$ sublevels. When $N \geq 2$, ${}^N\underline{\rho}(t_0)$, which is a $(2N+1)\times(2N+1)$ anisotropic matrix, is a function of $N+1 > 2$ parameters, and the following argument is no longer valid.

The absolute intensities of the resonances are given by (4). Let us calculate $\rho(t)$ using (5). We have

$${}^{N=1}\underline{\rho}(t_0) = \begin{pmatrix} Q_1 & 0 & 0 \\ 0 & Q_0 & 0 \\ 0 & 0 & Q_1 \end{pmatrix} nv = {}^1\rho^{(00)}{}^0_0\,\underline{T}^0_0 + {}^1\rho^{(00)}{}^2_0\,\underline{T}^2_0,$$

with

$${}^1\rho^{(00)}{}^0_0 = \frac{1}{\sqrt{3}}(Q_0 + 2Q_1)nv$$

and

$${}^1\rho^{(00)}{}^2_0 = \frac{2}{\sqrt{6}}(Q_1 - Q_0)nv,$$

where nv is the flux of the incident electron beam and ρ is defined in Paper I.[1] Using the relation $\underline{U}\,\underline{T}^{(0)}_0\,\underline{U}^\dagger = \underline{T}^{(0)}_0$ due to the unitarity of $\underline{U}$, we obtain

$$\underline{\rho}(t) = {}^1\rho^{(00)}{}^0_0\,\underline{T}^0_0 + {}^1\rho^{(00)}{}^2_0\,\underline{F}(\chi, t).$$

Then (4) becomes

$$I(\vec{u},\lambda) = I_0(Q_0+2Q_1)\frac{nv}{3\Gamma}\,\mathrm{Tr}\,\left|(\underline{e}_{\vec{u},\lambda}\cdot\underline{D})(\underline{e}_{\vec{u},\lambda}\cdot\underline{D})\right| + I_0(Q_1-Q_0)I_{\vec{u},\lambda}(\chi,t)\ .$$

The first term of this sum is independent of the applied magnetic fields and gives a constant base line at fixed electron beam intensity. Experimentally the electron beam intensity varies with the static magnetic field which introduces a field-dependent base line (see Sec. II). The second term represents the intensity of the resonances and is proportional to $(Q_0 - Q_1)$ which is the same for each resonance. Therefore, we carry out the calculation for the simple case where $Q_0 = 1$ and $Q_1 = 0$, and obtain

$$\rho_{ii} \propto \sum_{M_S} \left| C^i_{M_S, M_N=0} \right|^2 .$$

[1] M. A. Marechal, R. Jost, and M. Lombardi, preceding paper, Phys. Rev. A 5, 732 (1972).
[2] J. Brossel and F. Bitter, Phys. Rev. 86, 308 (1952).
[3] W. E. Lamb, Phys. Rev. 105, 559 (1957).
[4] I. Wieder and W. E. Lamb, Phys. Rev. 107, 125 (1957).
[5] F. O. Colegrove, P. A. Franken, R. R. Lewis, and R. A. Sands, Phys. Rev. Letters 3, 420 (1969).
[6] P. Baltayan and O. Nédélec, Phys. Letters 37A, 31 (1971).
[7] O. Nédélec and P. Baltayan, J. Phys. B 3, 1646 (1970).
[8] M. Lombardi, J. Phys. Radium 30, 631 (1969).
[9] L. Y. Chow Chiu, Phys. Rev. 137, 384 (1964).
[10] G. Herzberg, *Spectra of Diatomic Molecules* (Van Nostrand, Princeton, N. J., 1950).
[11] P. R. Fontana, Phys. Rev. 125, 220 (1962).
[12] C. Cohen-Tannoudji, Ann. Phys. (Paris) 7, 469 (1962).
[13] A. Messiah, *Mécanique Quantique*, (Dunod, Paris, 1964), p. 621.
[14] I. C. Percival and M. J. Seaton, Phil. Trans. Roy. Soc. London, A251, 113 (1958).
[15] W. Lichten, Phys. Rev. 126, 1020 (1962).
[16] J. P. Descoubes, thesis (University of Paris, 1967) (unpublished).

PHYSICAL REVIEW A VOLUME 5, NUMBER 2 FEBRUARY 1972

Excitation of Lithium by Electron Impact Using the Glauber Theory

K. C. Mathur, A. N. Tripathi, and S. K. Joshi
Physics Department, University of Roorkee, Roorkee, India
(Received 4 March 1971; revised manuscript received 10 May 1971)

The Glauber approximation has been applied to calculate the excitation cross section for the $2s$-$2p$ transition in lithium by electron impact using the frozen-core approximation. The integrated inelastic cross section has been compared with other theoretical calculations and with the experimental data. With this frozen-core, effectively one-electron formulation of electron-lithium excitation, it is found that the Glauber approximation provides better agreement with experimental data than the Born approximation.

I. INTRODUCTION

The Glauber approximation has been widely applied in studying the scattering problems in nuclear and particle physics.[1] Recently, this approximation was employed by Franco[2] in order to study the elastic scattering of electrons by hydrogen and helium. Tai *et al.*[3] and Ghosh *et al.*[4] have used this approximation to study the excitation of hydrogen by electron impact. The success of the Glauber theory in electron-atom collisions can be ascribed to the fact that it takes into account the interaction of the incident electron with the target electrons and protons, whereas in the usual approximations the interaction between the incident electron and the target proton produces a zero scattering cross section, as in the first Born approximation, or else a negligible scattering cross section, as in the impulse approximation.

In the present paper we have used the Glauber approximation to study the inelastic scattering of electrons by lithium atoms. Here we have assumed the lithium atom to behave like a one-electron system. The effect of the core electron has been ignored by adopting the frozen-core approximation. Thus, with this approximation we have only to evaluate a five-dimensional integral instead of an eleven-dimensional integral $(3Z+2)$ for the scattering amplitude.

II. THEORY

The scattering amplitude for the transition of an atom from an initial state i to a final state f is given by

$$F_{fi}(\vec{q}) = \frac{iK_i}{2\pi}\int \Phi_f^*(\vec{r})\Gamma(\vec{b},\vec{r})\Phi_i(\vec{r})e^{i\vec{q}\cdot\vec{b}}d^2b\,d\vec{r}\ , \quad (1)$$